

Coherent Atomic Beam Splitter Using Transients of a Chaotic System

A. G. Truscott, M. E. J. Friese, W. K. Hensinger, H. M. Wiseman, H. Rubinsztein-Dunlop, and N. R. Heckenberg

Department of Physics, Centre for Laser Science, The University of Queensland, Brisbane, Qld 4072 Australia

(Received 28 July 1999)

A coherent atomic beam splitter can be realized using the transient dynamics of a chaotic system. We have experimentally observed such an effect using ultracold rubidium atoms. Our experimental results are in good agreement with numerical simulations of the Schrödinger equation for the system.

PACS numbers: 03.75.Be, 32.80.Lg

Atomic beam splitters are essential elements in the field of atom optics. As in classical optics, it is necessary to be able to split atom waves in order to measure coherence effects. The applications of such devices are wide ranging and include atom interferometry [1,2], input/output couplers for atomic cavities [3], and state selective elements [4]. To date, successful splitting of an atomic wave function has been achieved using Raman pulses [2], a magneto-optical beam splitter [5,6], diffraction from an optical standing wave [7–9], adiabatic population transfer [10], optical Stern-Gerlach effect [11], and freestanding transmission structures [12]. More recently, coherent splitting of a Bose-Einstein condensate (BEC) has been achieved with optically induced Bragg diffraction [13] and with a pulsed standing light wave [14].

In this paper we show that the transient dynamics of an atom in a modulated standing wave (a chaotic system) can be used to split a cold atomic ensemble. Our beam splitter exhibits an unusual property, in that the resulting narrow outputs are highly dependent on the dynamics of the atoms themselves. For an ultracold sample of rubidium atoms prepared in a magneto-optic trap (MOT) we have achieved splittings of up to ± 70 photon recoils. Quantum mechanical simulations show that, for a source of atoms cooled to the recoil limit, the beam splitter outputs have the same velocity width as the source and contain up to 30% of the original atoms. Furthermore, the potential used is far detuned and is present only for a few microseconds so decoherence due to spontaneous emission is negligible. Since the atom-light interactions are conservative, and only one level of the atom is significantly populated, the beam splitting process is coherent.

To understand how a time dependent potential can split an atomic wave function into discrete momentum states, it is informative to consider the well known effect of diffraction of an atomic beam from a standing wave [15]. In such experiments, atoms with a small transverse velocity spread impinge on an optical standing wave and are diffracted into different momentum states. For diffraction to occur the interaction time must be small or oscillations of the atoms in the potential become relevant, a phenomenon sometimes called channeling. All diffraction experiments of this nature are thus restricted to the Raman-Nath region in which the change in kinetic energy of the atom under

the influence of a potential V is much smaller than V . For an optical standing wave, the potential near the bottom of a well can be approximated by a harmonic potential. In such a case the interaction time would need to be much less than a quarter of the classical period of oscillation for the system to be in the Raman-Nath regime. An alternative to such a scheme is to use an atomic ensemble with almost zero average momentum and pulse on an optical standing wave for a very short time (much less than a quarter of the classical period of oscillation). In either case the resulting atomic momentum distribution exhibits many broad peaks.

In contrast to the above beam splitter, ours operates outside the Raman-Nath regime and directly relies on the atomic motion during the interaction interval to split the atomic wave function. Also, we sinusoidally modulate the intensity of the optical standing wave as opposed to pulsing the standing wave. The end result is a robust beam splitter which is simple to achieve experimentally and has outputs with momentum spread of the same order as that of the input.

The system can be modeled by considering a two level atom, rubidium in our case, in a far detuned standing wave. For a sufficiently large detuning ($\delta_L \gg \Gamma/2\pi = 6.0$ MHz) the excited state can be adiabatically eliminated, resulting in a Hamiltonian for the ground state given by

$$H = P_x^2/2m - (\hbar\Omega_{\text{eff}}/8)(1 + 2\varepsilon \sin\omega_m t) \cos(2k_L x),$$

where the effective Rabi frequency is $\Omega_{\text{eff}} = \Omega^2/\delta_L$, $\Omega = \Gamma\sqrt{I/I_{\text{sat}}}$ is the resonant Rabi frequency, $I_{\text{sat}} = 1.65$ mW/cm² is the saturation intensity of the transition, Γ is the natural linewidth of the transition, ε is the depth of the modulation, ω_m is the modulation angular frequency, and k_L is the laser light wave number. To get an understanding of our beam splitter we first turn to a classical description of the dynamics. Applying Hamilton's equations from the above Hamiltonian gives the trajectories of atoms through phase space. For beam splitting to occur the effective Rabi frequency of the system is adjusted so that the harmonic frequency of atomic oscillations is approximately 0.6 of the driving frequency. The harmonic frequency is given by $\omega_h = \Gamma k_L \sqrt{(\hbar I/I_{\text{sat}})/2m\delta_L}$. Under such conditions the phase space trajectories of an atom initially at rest as a function of its starting position are shown in Fig. 1

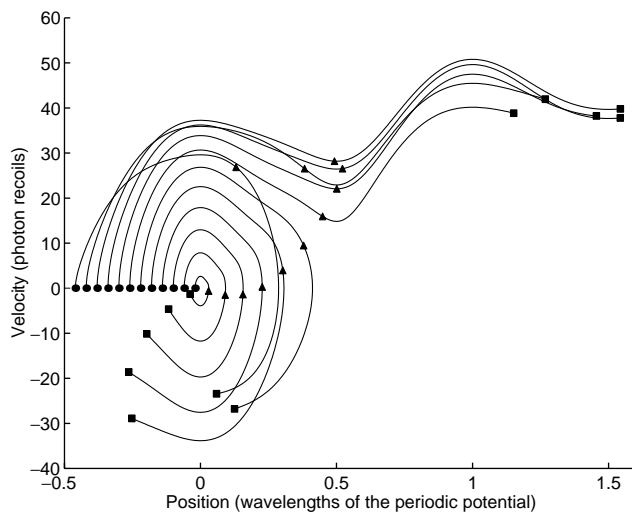


FIG. 1. Phase space trajectories of atoms that interact with a modulated standing wave. The interaction time of the atom with the potential is 1.75 cycles of the modulation period and we have used $\omega_m/2\pi = 450$ kHz, $\delta_L/2\pi = 44.5$ GHz, $I = 38.1$ W/cm², and $\varepsilon = 0.3$. The initial positions of the atoms in phase space are marked with circles, the positions after 1 cycle are marked with triangles, and the final positions after 1.75 cycles are marked with squares.

(for clarity we have plotted only the atomic trajectories for negative starting positions). The interaction time of the atom with the potential is 1.75 cycles of the modulation period and we have used $\omega_m/2\pi = 450$ kHz, $\delta_L/2\pi = 44.5$ GHz, $I = 38.1$ W/cm², and $\varepsilon = 0.3$. The initial positions of the atoms in phase space are marked with circles, the positions after 1 cycle are marked with triangles, and the final positions after 1.75 cycles are marked with squares. From Fig. 1 it is clear that after one period of the modulation there is a large group of atoms that have arrived at a maximum of the potential. Also, since one modulation cycle has passed the potential has returned to its original height and is about to rise again. Thus this group of atoms is in the perfect position to “surf” the potential, which results in the atoms gaining a large amount of kinetic energy. In fact, by the end of the interaction these atoms have traveled almost one and a half periods of the potential. More importantly, their final velocities form a narrow band in velocity space. Although we have examined the case of an atom initially at rest to describe the beam splitting process, it turns out that the phase space trajectory map for atoms starting with up to six photon recoils of velocity looks very similar to that of Fig. 1, the only notable difference being a larger spread in final velocity for the group of atoms that escape from the initial potential well. It should also be noted that the beam splitting process is destroyed for longer interaction times, due to the nonlinearity of the system.

Until this point our analysis and discussion have been entirely classical, while atomic beam splitting is a quantum mechanical effect. To quantum mechanically simulate the system we solve Schrödinger’s equation for a state vector of the form $|\psi\rangle = \sum_{n=-m,m} c_n |2n\hbar k_L\rangle$. This yields

a set of coupled differential equations in the momentum probability amplitudes c_n . In the absence of spontaneous emission the proportion of atoms in the n th momentum state is given by $|c_n|^2$. In the regime studied we estimate the chance of an atom absorbing a photon to be less than 1 part in 100, thus neglecting spontaneous emission is a reasonable approximation.

An excellent test of the beam splitter is to apply it to an ensemble of atoms prepared in a MOT. By loading an optical standing wave with the MOT output and applying the correct intensity modulation it should be possible to split the initial velocity distribution of the atomic cloud.

Our experimental setup consists of about 10^6 rubidium atoms prepared in a MOT. The $1/e$ velocity full width of the MOT distribution is approximately 13 recoil velocities. After the final cooling stage, the MOT is turned off but the repumping beam is left on, forcing the accumulation of atoms in the $F = 3$ ground state. We allow an optical pumping period of approximately 500 μ s after which the interaction potential is switched on. A frequency stabilized titanium sapphire (Ti-S) laser is used to produce the optical standing wave. The output of the Ti-S laser is spatially filtered using a polarization preserving single mode optical fiber and intensity stabilized to better than 1%. Temporal modulation of the optical potential is achieved using an acousto-optic modulator which is driven by a voltage signal from an arbitrary wave form generator. After the interaction the atoms undergo a free expansion interval, until the molasses beams are once again turned on, freezing the atoms’ positions and allowing detection [16,17]. We used a standing wave with a $1/e$ Gaussian width of 2.2 mm in these experiments, which when combined with the initial width of the MOT of 400 μ m gives a maximum variation in intensity of 4% over the spatial extent of our cloud.

To determine the momentum of the beam splitter outputs, we plot their position versus ballistic expansion time, for a series of increasing ballistic intervals up to 12 ms. Linear regression on this line provides an estimate of their momentum to better than 3%. This value is assigned to the center of the peaks and thus scales the momentum axis. Figure 2 shows the experimental momentum distribution (solid line) of atoms that have interacted with 1.75 cycles of a $\omega_m/2\pi = 450$ kHz, $I = 40.6 \pm 5$ W/cm², $\delta_L/2\pi = 44.5$ GHz interaction potential. Also shown in Fig. 2 is the predicted momentum distribution based on a quantum mechanical simulation (dotted line) of the system. To obtain theoretical momentum distributions we convolve the calculated momentum distribution with the appropriately scaled MOT initial spatial distribution. As is seen in Fig. 2 our experimental results are in good agreement with theoretical simulations. The momentum of the beam splitter outputs, as well as the number of atoms in each output, is predicted well by our quantum mechanical model. Interestingly, numerical calculations show that the $1/e$ velocity width of the beam splitter outputs, for these parameters, is approximately five photon recoils, almost a factor of 3 colder than the

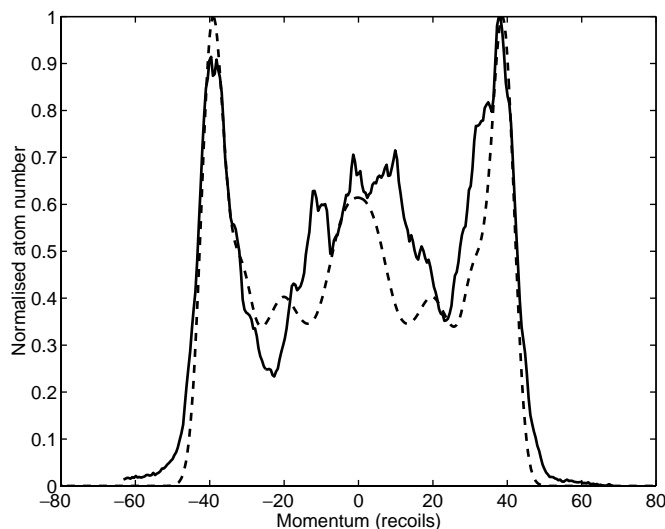


FIG. 2. Experimental momentum distribution (solid line) of atoms that have interacted with 1.75 cycles of a $\omega_m/2\pi = 450$ kHz, $I = 40.6 \pm 5$ W/cm², $\delta_L/2\pi = 44.5$ GHz interaction potential. Also shown is the predicted momentum distribution based on a quantum mechanical simulation (dotted line) of the system.

beam splitter input. Experimentally we can estimate the velocity spread of these outputs by plotting their widths versus ballistic expansion time, for a series of increasing ballistic intervals. Using this method we have confirmed that the beam splitter outputs are colder than the MOT input. However, this time of flight technique is limited by the initial spatial width of the outputs and cannot give an accurate measure of the velocity spread of the beam splitter outputs.

By varying the modulation frequency and subsequently correcting the effective Rabi frequency to observe beam splitting, we have been able to create side peaks traveling at velocities up to ± 70 photon recoils. We recorded the laser detuning required to maximize the number of atoms in the beam splitter output for a given modulation frequency and intensity. The number of atoms was sensitive to changes in detuning of around 200 MHz. The error bars shown are determined from the estimated errors in the laser intensity and detuning. The results of these measurements are plotted in Fig. 3 in the form of ω_h versus ω_m . The slope of this graph gives the ratio of the harmonic frequency to the modulation frequency at which the beam splitting effect occurs. Our measurements show that beam splitting occurs when the system is driven at 0.57 ± 0.02 of its harmonic frequency, in agreement with our model.

It should be noted that the beam splitter presented here uses a completely different effect than the recently reported phase space resonances [18]. Such resonances are long term effects (usually taking 4 or 5 cycles of the modulation to appear) and occur when the harmonic frequency is approximately equal to the driving frequency of the system. Most importantly, phase space resonances are localized in both position and momentum and thus have a relatively large momentum spread.

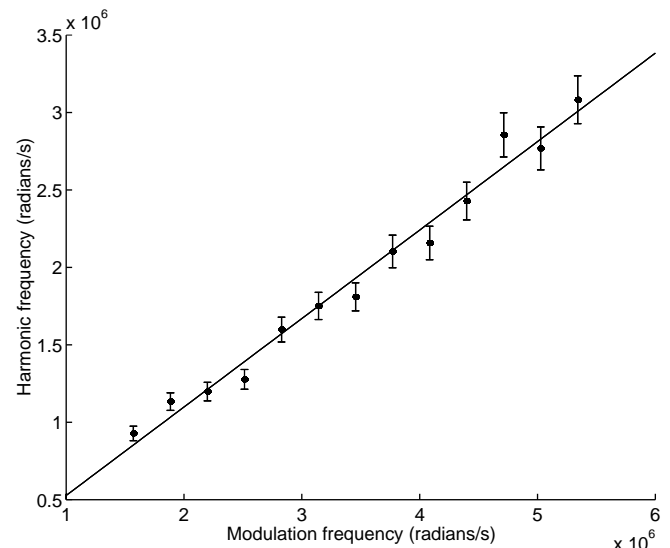


FIG. 3. Graph of ω_h versus ω_m . The slope of this graph gives the ratio of the harmonic frequency to the modulation frequency for which beam splitting occurs.

We now turn our attention to analyzing our beam splitter's performance. In particular, we want to consider the case for which the input to the beam splitter is coherent, i.e., an ensemble of atoms cooled to the recoil limit. For our simulations we choose the following modulation parameters: $\omega_m/2\pi = 250$ kHz, $I = 35.9$ W/cm², $\delta_L/2\pi = 141.5$ GHz, $\epsilon = 0.35$, and we set the interaction time to be 1.75 cycles of the modulation frequency. For comparison we also simulate a beam splitter that uses an unmodulated standing wave which is only turned on for a short period of time and operates in the Raman-Nath regime, as was described earlier. The results of these simulations are shown in Figs. 4(a) and 4(b), respectively. For the parameters used both the resulting momentum distributions are peaked around ± 22 photon recoils. However, for the case of the transient beam splitter the outputs are much narrower and contain around twice the number of atoms. In fact, the width of the transient beam splitter output is about one photon recoil, i.e., the same as the input width. Clearly the transient beam splitter has better output characteristics than simple diffraction from a periodic potential. Furthermore, the outputs of the transient beam splitter are easily tunable. By choosing the appropriate modulation frequency the momentum of the beam splitter outputs can be varied. For higher modulation frequencies the beam splitter outputs have much larger momentum. This increase in output momenta comes at the cost of efficiency. An example of this is shown in Fig. 4(c) where we have simulated the system for the following modulation parameters: $\omega_m/2\pi = 650$ kHz, $I = 33.9$ W/cm², $\delta_L/2\pi = 20.7$ GHz, $\epsilon = 0.4$. For such a modulation the momentum distribution is peaked around ± 58 recoils and contains around 10% of the input atoms in each output. We show the corresponding case for an unmodulated standing wave in Fig. 4(d).

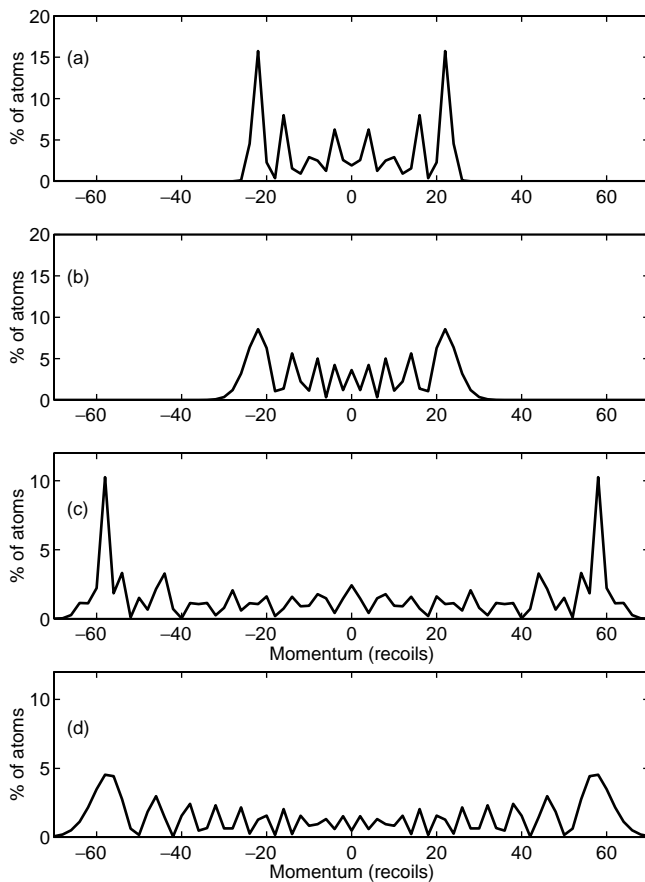


FIG. 4. Theoretical momentum distributions obtained from simulating the following systems: (a) a transient beam splitter with parameters $\omega_m/2\pi = 250$ kHz, $I = 35.9$ W/cm², $\delta_L/2\pi = 141.5$ GHz, $\varepsilon = 0.35$, and an interaction time of 1.75 modulation cycles; (b) an unmodulated standing wave which is turned on only for a short period of time and operates in the Raman-Nath regime; (c) a transient beam splitter with parameters $\omega_m/2\pi = 650$ kHz, $I = 33.9$ W/cm², $\delta_L/2\pi = 20.7$ GHz, $\varepsilon = 0.4$; and (d) corresponding unmodulated standing wave case of (c).

A natural question to ask is if this novel beam splitter could be used to construct an atom interferometer. Since the transient beam splitter relies on the dynamics of the atoms, the effect is dependent on the input momentum distribution. While this beam splitter can split any single component momentum distribution, it cannot split a complicated superposition of momentum states in the same way as diffraction from a matter grating [12]. However, the transient beam splitter can be applied “backwards,” by reversing the phase of the modulation. We have modeled this effect, and our simulations show that when the beam splitter with modulation phase reversed is applied to the original outputs after a time delay, the outputs return to the zero momentum state. This means that we now have two outputs with zero momentum that are spatially separated, opening up the possibility for atom interferometry.

In summary, we have demonstrated an atomic beam splitter that uses a mechanism completely different from

all previously studied, namely, the transients of a chaotic system. The method is simple to implement experimentally, relying only on accurate control of the light intensity. When the scheme is applied to a MOT distribution we find that up to 30% of the atoms are in each beam splitter output, in good agreement with theoretical simulations. We have also theoretically studied the case for which the beam splitter acts on recoil cooled atoms. For such a case we find that the beam splitter outputs are also recoil limited and each contain up to 16% of the original atoms. Moreover, by changing the modulation parameters one can tune the momentum of the outputs. Finally, the method may be suitable for manipulating BEC. In particular, it might be useful as an output coupler for an atom laser.

This work is supported by the Australian Research Council.

-
- [1] D.W. Keith, C.R. Ekstrom, Q.A. Turchette, and D.E. Pritchard, *Phys. Rev. Lett.* **66**, 2693 (1991).
 - [2] M. Kasevich and S. Chu, *Phys. Rev. Lett.* **67**, 181 (1991).
 - [3] D.E. Pritchard, *Atom Optics, Proceedings of the Twelfth International Conference on Atomic Physics* (AIP, New York, 1990).
 - [4] M. Kasevich, D.S. Weiss, E. Riis, K. Moler, S. Kasapi, and S. Chu, *Phys. Rev. Lett.* **66**, 2297 (1991).
 - [5] T. Pfau, C. Kurtsiefer, C.S. Adams, M. Sigel, and J. Mlynek, *Phys. Rev. Lett.* **71**, 3427 (1993).
 - [6] C.S. Adams, T. Pfau, C. Kurtsiefer, and J. Mlynek, *Phys. Rev. A* **48**, 2108 (1993).
 - [7] P.E. Moskowitz, P.L. Gould, S.R. Atlas, and D.E. Pritchard, *Phys. Rev. Lett.* **51**, 370 (1983).
 - [8] P.L. Gould, G.A. Ruff, and D.E. Pritchard, *Phys. Rev. Lett.* **56**, 827 (1986).
 - [9] M.K. Oberthaler, R. Abfalterer, S. Bernet, C. Keller, J. Schmiedmayer, and A. Zeilinger, *Phys. Rev. A* **60**, 456 (1999).
 - [10] M. Weitz, B.C. Young, and S. Chu, *Phys. Rev. Lett.* **73**, 2563 (1994).
 - [11] T. Sleator, T. Pfau, V. Balykin, O. Carnal, and J. Mlynek, *Phys. Rev. Lett.* **68**, 1996 (1992).
 - [12] D.W. Keith, M.L. Schattenburg, H.I. Smith, and D.E. Pritchard, *Phys. Rev. Lett.* **61**, 1580 (1988).
 - [13] M. Kozuma, L. Deng, E.W. Hagley, J. Wen, R. Lutwak, K. Helmerson, S.L. Rolston, and W.D. Phillips, *Phys. Rev. Lett.* **82**, 871 (1999).
 - [14] Yu. B. Ovchinnikov, J. H. Müller, M. R. Doery, E. J. D. Vredenburg, K. Helmerson, S. L. Rolston, and W. D. Phillips, *Phys. Rev. Lett.* **83**, 284 (1999).
 - [15] P. J. Martin, P. L. Gould, B. G. Oldaker, A. H. Miklich, and D. E. Pritchard, *Phys. Rev. A* **36**, 2495 (1987).
 - [16] F. L. Moore, J. C. Robinson, C. F. Bharucha, Bala Sundaram, and M. G. Raizen, *Phys. Rev. Lett.* **75**, 4598 (1995).
 - [17] A. G. Truscott, D. Baleva, N. R. Heckenberg, and H. Rubinsztein-Dunlop, *Opt. Commun.* **145**, 81 (1998).
 - [18] A. G. Truscott, W. K. Hensinger, M. Hug, M. E. J. Friese, H. Rubinsztein-Dunlop, N. R. Heckenberg, and G. J. Milburn (to be published).